SIMULATION OF MEASURED SEAFLOOR ROUGHNESS SPECTRUM TIME SERIES USING A COUPLED RIPPLE-BIOTURBATION MODEL

A Penko Naval Research Laboratory, Stennis Space Center, MS, USA
S Johnson Pennsylvania State University, Applied Research Lab., State College, PA, USA
J Calantoni Naval Research Laboratory, Stennis Space Center, MS, USA

1. INTRODUCTION

The seafloor boundary layer is a complex environment affected by hydrodynamic, biologic, and anthropogenic processes. For example, ripple formation by waves and ripple degradation from biological activity are opposing forces occurring continuously on the seafloor. Seafloor roughness caused due to the presence of bottom features (e.g., ripples, fish pock marks) and bottom sediments (e.g., sand, gravel) affect the acoustic scattering and penetration properties of the seafloor. Therefore, a model that will forecast the growth and decay of ripples as well as the evolution of the seafloor roughness due to bioturbation may provide critical inputs for acoustic penetration and scattering models. Many existing ripple predictors assume that the seafloor is in equilibrium with the wave forcing and rarely take into account any diffusive or biological effects. Additionally, the length scales of seafloor characteristics are typically described and modeled using scalar quantities such as a mean grain size (d_{50}) or single ripple length (λ) and height (η). However, often in nature there exist many length scales ranging from a distribution of sediment sizes to three-dimensional ripples of multiple lengths and heights oriented in different directions. The seafloor effects on the hydrodynamics of the flow (and vice versa) are most strongly dependent on the size of the bottom features. Representing the seafloor surface in wavenumber space allows for the inclusion of the seafloor boundary layer interactions over a range of length scales. Modeling the seafloor spectrum can therefore provide information about features O(mm) to O(m) (i.e., grains to ripples) that can be coupled with oceanographic and acoustic models.

A composite spectral / procedural seafloor model is proposed that predicts the spatial and temporal evolution of seafloor roughness accounting for both the formation and degradation of ripples due to waves and biology. The system couples a time-dependent spectral ripple model (Traykovski, 2007; Nelson and Voulgaris, 2015) with a bioturbation model that restores the random roughness equilibrium. (Jackson et al, 2009; Johnson and Lyons, 2011, Johnson and Jackson, 2015). The coupled model system predicts a time series of the roughness spectrum given the sediment type and a time series of wave conditions. The model predictions are compared qualitatively to field observations of spectral evolution.

2. MODEL DESCRIPTIONS

Following Jackson et al. (2009), we model the temporal evolution of seabed relief as

$$\mathrm{f}(\mathbf{r},t) = \mathrm{f}_r(\mathbf{r},t) + \mathrm{f}_b(\mathbf{r},t)$$

where f_r is the ripple component and includes both a growth and decay term, f_b is the bioturbation component, $\mathbf{r}$ is a 2D position vector (i.e., $\mathbf{r} = \sqrt{x^2 + y^2}$), and t is the time. When the wave conditions are energetic and the bottom shear stress is above a given threshold, the hydrodynamic forces dominate ($O(\mathrm{f}_r) \gg O(\mathrm{f}_b)$) and the bioturbation can be neglected. When the wave conditions are low and the bottom shear stress is below a given threshold, both hydrodynamic and biological forces are of the same order of magnitude ($O(\mathrm{f}_r) = O(\mathrm{f}_b)$) and the random roughness generated

from bioturbation must be taken into account. The two models for ripple evolution and bioturbative random roughness evolution are presented in Sections 2.1 and 2.2, respectively.

2.1 Spectral Ripple Model

The spectral ripple model builds on previous models developed to predict sand ripple evolution (Traykovski, 2007; Nelson and Voulgaris, 2015). The time-dependent model describes the temporal evolution of the seafloor spectra components as a relaxation process. The rate of change of the seafloor spectrum is described by

$$\frac{dS_\eta(k,t)}{dt} = \frac{S_{\eta,eq}(k,t) - S_\eta(k,t)}{T_k(k,t)} \quad (1)$$

where k=2π/λ is the wavenumber vector, $S_\eta(k,t)$ is the seafloor spectrum at time t, the subscript eq denotes equilibrium, and T_k is the adjustment time for each ripple wavenumber. The adjustment time is based on the cross-sectional area of the ripple and the volumetric sediment transport rate, Q, and is given by

$$T_k(k,t) = \alpha(1-\phi)0.16(2\pi/k)^2/(2Q), \quad (2)$$

where ϕ is the sediment porosity (0.4) and α is an empirical time constant. The Meyer-Peter and Müller (1948) formulation is used to calculate the volumetric sediment transport rate,

$$Q = \begin{cases} \gamma(\theta-\theta_{cr})^{1.5}\sqrt{(S-1)gd_{50}^3} & \theta \geq \theta_{cr} \\ 0 & \theta < \theta_{cr} \end{cases}, \quad (3)$$

where $\theta = 0.5 f_w u_b^2/[(S-1)gd_{50}]$, is the Shields parameter, f_w is the friction factor (Swart, 1976), u_b is the wave orbital velocity at the bed, S is the sediment specific gravity, and θ_{cr} is the critical value for sediment motion. The model assumes the ripples are being driven to the equilibrium spectrum for the instantaneous wave conditions. The equilibrium spectrum is generated from a Gaussian distribution of the equilibrium ripple height (η_{eq}) and length (λ_{eq}) (Traykovski, 2007),

$$S_{\eta,eq}(k,t) = \frac{0.25\eta_{eq}}{\sigma\sqrt{2\pi}}\exp\left[-0.5\left(\frac{k-k_{eq}}{\sigma}\right)^2\right]^{\frac{1}{2}} \quad (4)$$

where σ is the spectral width of the distribution and represents the range of existing ripple wavelengths. The spectral width is set to π/2 based on observed seafloor spectra. The equilibrium ripple height and length are calculated from the equilibrium ripple predictor of Nielson (1981) given by

$$\eta_{eq} = \begin{cases} A_b\left(0.275 - 0.022\varphi^{0.5}\right) & \varphi \leq 10 \\ A_b\left(21\varphi^{-1.85}\right) & \varphi > 10 \end{cases}, \quad (5)$$

$$\lambda_{eq} = \eta_{eq}\Big/\left(0.342 - 0.34\theta^{0.25}\right), \quad (6)$$

where $\varphi = 2\theta/f_w$ is the mobility number. The model predicts the seafloor to exist in one of three states using estimated bottom shear stress based on two threshold conditions for the Shields parameter, θ. The threshold conditions include the critical value for sediment motion, θ_{cr} = 0.05, of

typical beach sand and the critical value for complete wash out, θ_{wo} (Soulsby et al., 2012). The critical value for complete wash out is a function of the grain size, density, and water viscosity,

$$\theta_{wo} = \begin{cases} 1.66 D_*^{-1.3} & D_* > 1.58 \\ 0.916 & D_* \leq 1.58 \end{cases} \quad (7)$$

where $D_* = [g(S-1)/\nu^2]^{\frac{1}{3}} d_{50}$, is the non-dimensional grain size diameter. If the Shields parameter is greater than the wash out threshold, sheet flow conditions exist and the model predicts an infinite ripple length and a ripple height of zero. When the Shields parameter is between the critical threshold for sediment motion (0.05) and the wash out threshold, the model spectra are evolved using (**1**). When the Shields parameter is less than the critical threshold for sediment motion, the ripple length remains constant and the biological model degrades the ripple height. The spectral decay due to bioturbation is approximated as a diffusive process and described with an exponential decay equation (Jackson et al., 2009)

$$S_\eta(k, t+\Delta t) = S_\eta(k,t) e^{-Dk^2 \Delta t} \quad \text{if} \quad \theta < \theta_{cr}, \quad (8)$$

Where Δt is the time step and D is the horizontal diffusion coefficient, which is site and sediment specific. The diffusion coefficient used here was determined from observations of backscatter intensity.

The spectral seafloor model was initialized with a ripple wavelength and height and forced with measured, in situ, time series of wave conditions. The spectral model assumes that each wave number component of seafloor spectra evolves independently. The seafloor spectra, ripple length and height, and sediment transport are output at every model time step, Δt = 30 min.

2.2 Bioturbation Simulation

Here we assume the forcing function that evolves the seabed from organized ripples to random roughness is caused by bioturbation, and will be modeled using Johnson et al., 2015. The model is a procedural generation technique whereby a biologically-inspired basis texture is applied stochastically to the seabed relief at a specified rate. The basis texture assumed is meant to model a fish feeding pit and is a 3D version of the second derivative of a Gaussian (also referred to as an (inverted) besinc, jinc, or sombrero function). It is subjected to the same diffusive process (8) as the seafloor spectra described in the previous section. An individual bioturbative event including diffusion is modeled as

$$g(\mathbf{r},t) = b\frac{a^4}{\tilde{a}^4}\left[\left(\frac{r}{\tilde{a}}\right)^2 - 1\right] e^{-(r/\tilde{a})^2} = \zeta \frac{a^5}{\tilde{a}^4}\left[\left(\frac{r}{\tilde{a}}\right)^2 - 1\right] e^{-(r/\tilde{a})^2} \quad (9)$$

where

$$\tilde{a}^2 = a^2 + 4Dt \quad (10)$$

The parameter *a* is pit radius, *b* is the pit depth, ζ is the pit slope, and *t* is the time. To create a realization of *n* events, the values of *a* and ζ (or *a* and *b*) are chosen as random variables, with the location of the pit also a random variable. For the discussion here, pit radius is Rayleigh-distributed (with a mean of 2.0 cm), and pit slope is beta distributed (and bounded such that the maximum slope of the pit does not exceed the angle of repose). While the realization is a procedural generation technique needs to be calculated for a specific point in time, the *equilibrium* roughness spectrum is given by

$$W(\mathbf{k}) = \frac{N\langle \zeta_n^2 \rangle}{128TL^2D} k^2 \int_0^\infty p(a_n) a_n^{10} e^{-k^2 a^2/2} da_n \qquad (11)$$

where N is the total number of pits, T is the time, L^2 is the area of the surface, D is the diffusion constant, ζ_n^2 is the expected value of the slope distribution, k^2 is the wavenumber magnitude, a_n is the pit radius, and $p(a_n)$ is the PDF of the radius distribution. With several free parameters, this model is able to fit a wide range of data. However, this flexibility requires a need for additional measures of the biology and environment. In lieu of these measures, reasonable parameters guided by physical intuition were chosen for the purposes of this discussion.

3. FIELD OBSERVATIONS

Wave conditions and the seabed were observed during the Target and Reverberation Experiment (TREX13) funded by ONR and SERDP. A quadpod with instrumentation collected data for 34 days (20 April – 23 May 2013) in 7.5 m depth offshore of Panama City, FL, USA. An AWAC recorded wave height and period every 30 min (Figure 1). The wave orbital velocities at the bottom were calculated using linear wave theory and the recorded significant wave height and wave period. The Shields parameter is calculated from the bottom orbital velocities and plotted in Figure 1 with the two Shields parameter thresholds, θ_{cr} and θ_{wo}. In order to investigate the evolution of the seafloor due to diffusive processes and bioturbation, we examine a time period during the end of the experiment (May 11 – 16) when the wave action was low ($\theta < \theta_{cr}$). The beginning of this time period (May 11) will be assumed to be *t=0* in the rest of the paper. The ripple model is forced with the times series of bottom velocities and observed wave periods from this time period. We compare the observed and predicted ripple length, height and spectra in Section 4.

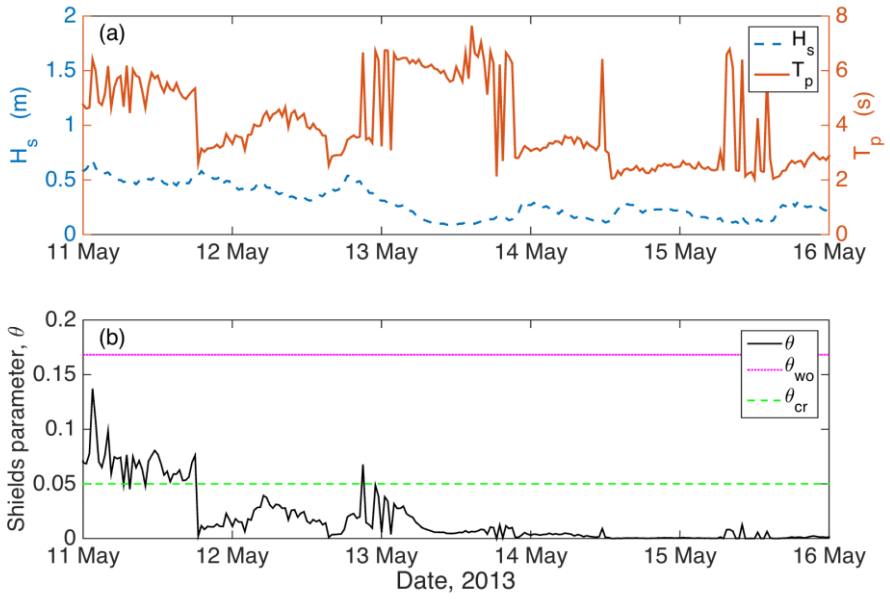

Figure 1: (a) Observed significant wave height (blue dashed line) and wave period (orange solid line) for the time period used in this paper. (b) Shields parameter calculated from observations with the critical value for sediment motion (green dashed line) and the critical value for ripple wash out (magenta dotted line).

To observe the seafloor, high-frequency (2.25 MHz) sector-scanning sonar imaged a small area (~15 square meters) under the quadpod every 12 minutes. The images provided backscatter intensity values throughout the experiment. A portion of each image was processed using 2D FFTs

to obtain the two-dimensional spectrum, S_o, of backscatter intensity. The observed ripple wavelength is calculated from the wave number corresponding to the spectral peak,

$$\lambda_o(t) = 2\pi/\sqrt{k_{x,peak}^2(t) + k_{y,peak}^2(t)}. \quad (12)$$

Since the images only provide backscatter and not elevation, we cannot directly extract ripple height (or decay time) from the spectra. However, a proxy for the observed ripple height can be calculated from the integral of the spectrum,

$$\eta_o(t) = \sqrt{\int\int S_o(k_x, k_y, t) dk_x dk_y}. \quad (13)$$

The image sequence provided high-resolution observations of ripple growth, decay, and reorientation under a wide range of forcing conditions to compare to the ripples predicted by the spectral seafloor model.

4. MODEL RESULTS

4.1 Ripple height and length

The spectral ripple model predicts the seafloor spectra (S_η) for every time, t. The predicted ripple height, η_p, and length, λ_p, are calculated from the predicted spectra, respectively as,

$$\eta_p(t) = 4\sqrt{\int S_\eta(k,t) dk} \quad (14)$$

$$\lambda_p(t) = 2\pi/k_m(t) \quad (15)$$

where the subscript p denotes predicted and k_m is the mean wavenumber of the spectrum at time, t. Comparisons of observed spectral intensity decay with predicted ripple height decay are plotted in Figure 2. The diffusion coefficient value $D = 5.6 \times 10^{-9}$ m^2/s was applied with good agreement. Both the model and observations have similar rates of decay and the diffusion coefficient is within the typical range observed at a nearby location (Jackson et al., 2009).

Ripple length comparisons between the model and observations are plotted in Figure 3. Due to the low wave action, the ripple length does not change significantly. Diffusion tends to only affect the ripple height and slope (Figure 2). The modeled mean ripple length is in good agreement with the observations. The modeled seafloor spectra (S_η) in wave length space ($\lambda = 2\pi/k$) is contoured in gray. Note the modeled spectra are multimodal from May 11-13. The multimodal spectra represent the existence of multiple ripple wavelengths, however, the model calculates the final predicted ripple length from the mean of the spectrum, resulting in a ripple length that is the mean of the two dominant wavenumbers.

Additionally, the coupling of the two models discussed previously permits investigations into not only the decay of the ripple component, but also the growing (to equilibrium) random roughness component due to bioturbative forcing (Section 4.2).

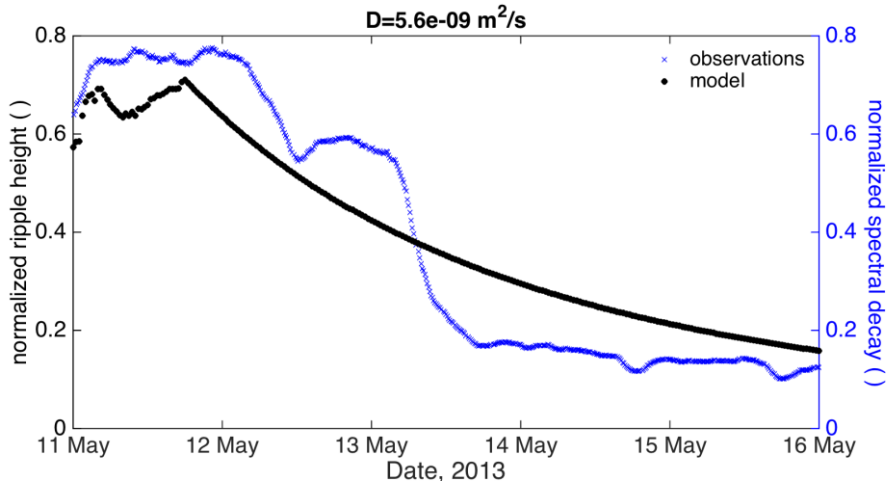

Figure 2: Normalized ripple height ($\eta_p/\eta_{p,max}$) predicted by the model (•) and the normalized spectral decay ($\eta_o/\eta_{o,max}$) from the observations (x).

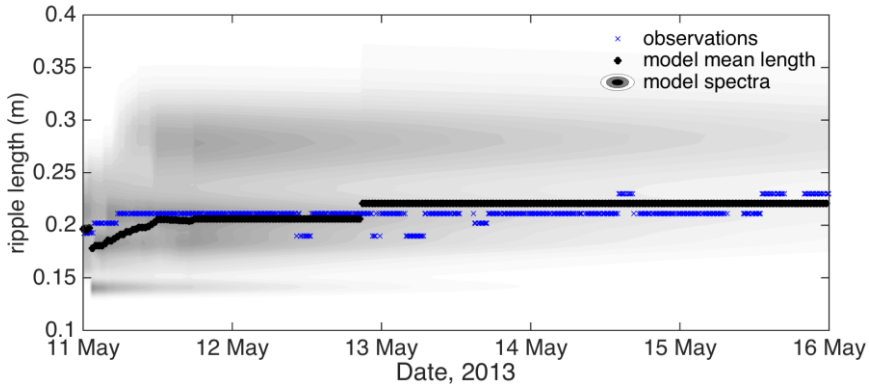

Figure 3: Ripple length predicted by the model (•) and calculated with spectral analysis from the sector scanning sonar images (x). Contoured is the modeled seafloor spectrum in wavelength space.

4.2 Composite Ripple and Bioturbation Spectra

The roughness spectra generated in the bioturbation simulation at three different times and a 2D FFT of the backscatter intensity recorded by the sonar at the same times is shown in Figure 4. The images at the three times are similar, illustrating the decay of the structure and the growth of the random roughness occurring due to bioturbation. Please note this comparison is qualitative only as the colorbars are not the same.

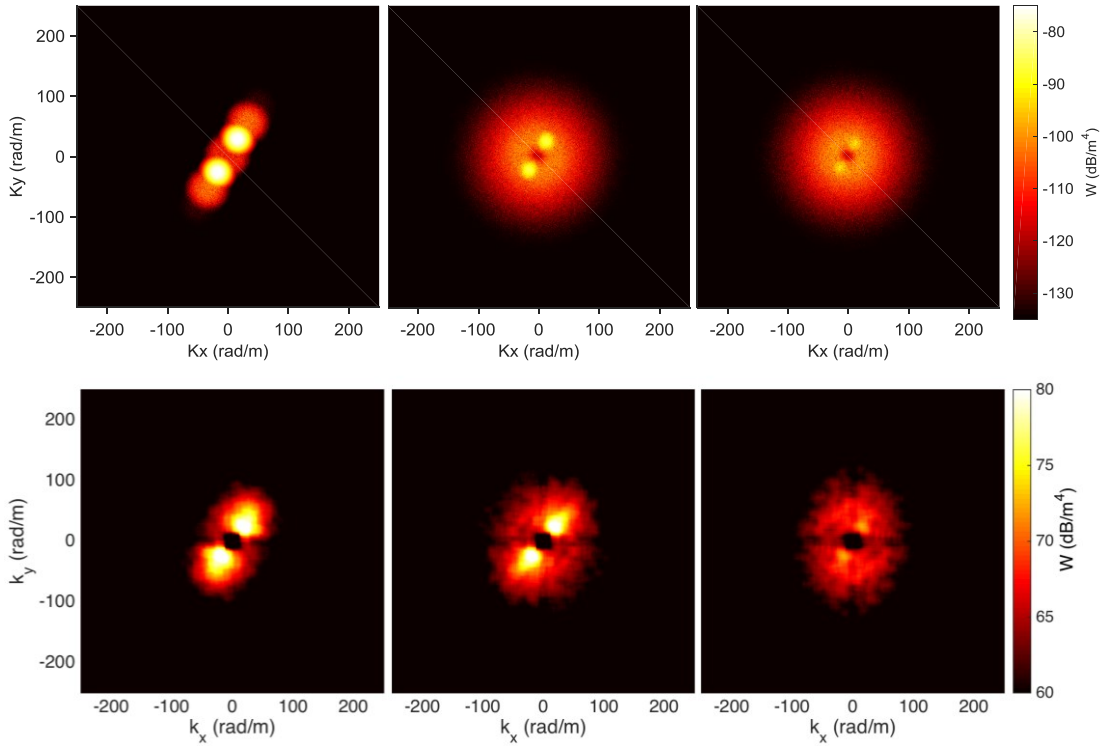

Figure 4: Roughness spectra for realization evolution from *t* = 0 days, *t* = 2.2 days, and *t* = 5.0 days (top, left to right). 2D power spectrum of the backscatter intensity from the sector scanning sonar on May 11 (t=0), 13 (t=2.2 days) and 16 (t=5 days) (bottom, left to right).

4.3 Simulating Acoustic Imagery

Seabed realizations were generated using the methods described here, and SONAR imagery was created using an adaptation of a sonar image simulator described in (Johnson and Lyons, 2010, 2011) for comparison to experimental imagery. Figure 5 (left) shows the evolution of simulated acoustic imagery as might be collected with a rotary fan beam sonar for the realizations of Figure 4 (top). Figure 5 (right) are the observed sonar images at equivalent times.

5. CONCLUSIONS

We presented a spectral ripple model to predict the temporally evolving seafloor spectra forced with an observed time series of wave height and period. The predictions of ripple length are in good agreement with the ripple length obtained from sonar images of backscatter intensity. A bioturbation model was also presented which allows for prediction of the growth of random roughness to equilibrium (assuming no additional evolution from hydrodynamic forcing of ripples occur). A qualitative comparison of realizations provided by the combination of ripple spectral model, a bioturbation procedural model, and a sonar simulation, to experimental sector scanning sonar images shows that the horizontal diffusion using the estimated diffusion coefficient and a representative bioturbative rate give similar acoustic responses. Additionally, the normalized predicted ripple height using the estimated diffusion coefficient and the normalized observed spectral energy decay are in good agreement. This work suggests that models for ripple evolution and bioturbation can provide a realistic forecast of the seafloor roughness evolution.

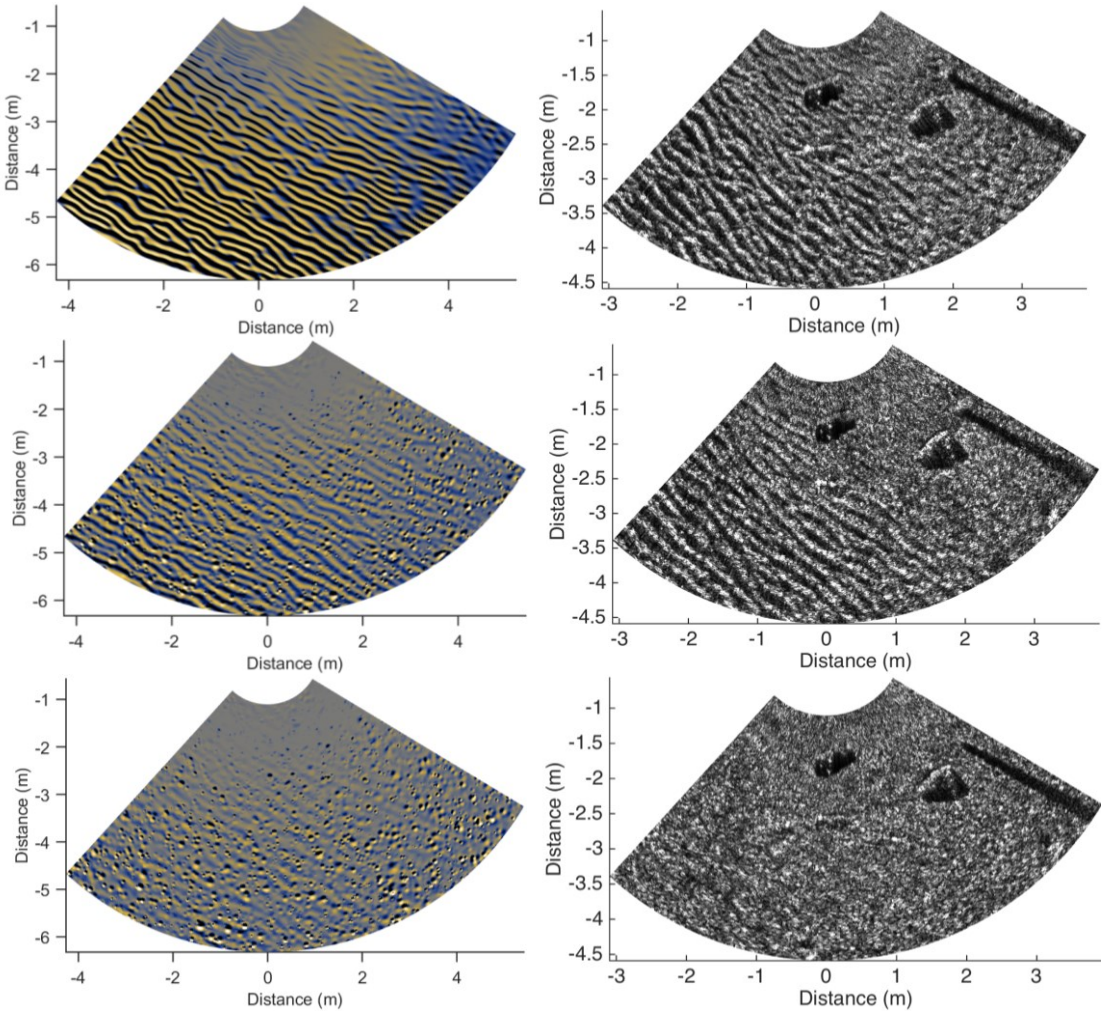

Figure 7: Simulated rotary fan beam imagery for example realization evolution of Figure 6, from t = 0 days (top left), t = 2.2 days (middle left), and t = 5.0 days (bottom left). Experimental sector scanning sonar images for May 11 (top right), May 13 (middle right), and May 16 (bottom right).

6. REFERENCES

1. P. Traykovski, 'Observations of wave orbital scale ripples and a nonequilibrium time-dependent model,' J. Geophys. Res., 112, C06026, (2007).

2. T. Nelson and G. Voulgaris, 'A spectral model for estimating temporal and spatial evolution of rippled seabeds,' Ocean Dynamics, 65, 155–171. (2015).

3. D. R. Jackson, M. D. Richardson, K. L. Williams, A. P. Lyons, Christopher D. Jones, K. B. Briggs, and D. Tang, 'Acoustic Observation of the Time Dependence of the Roughness of Sandy Seafloors,' IEEE Journal Of Oceanic Engineering, 34, 4. (2009).

4. S.F. Johnson and A.P. Lyons, 'Simulation of Rippled-Sand Synthetic Aperture Sonar Imagery,' Proceedings of The Institute of Acoustics International Conference on Synthetic Aperture Radar and Sonar, Lerici, Italy. (2010).

5. S.F. Johnson and A.P. Lyons, 'Simulation of rippled-sand seafloor evolution for synthetic SAS imagery,' Proceedings of the 4th Underwater Acoustic Measurements Conference, Technologies and Results, Kos, Greece. (2011).

6. S.F. Johnson and D.R. Jackson, 'Modelling seafloor bioturbation,' Proceedings of the Institute of Acoustics Seabed and Sediment Acoustics: Measurements and Modelling, Bath, United Kingdom. (2015).

7. D. H. Swart, 1976. 'Predictive Equations Regarding Coastal Transports.' Proceedings of 15th Coastal Engineering Conference, II, Honolulu. Hawaii. ASCE, New York City, New York State, 1113–1132. (1976).

8. P. Nielsen, 'Dynamics and geometry of wave-generated ripples.' J. Geophys. Res. 86 (C7), 6467–6472. (1981).

9. Soulsby, R.L., Whitehouse, R.J.S., Marten, K.V., 'Prediction of time-evolving sand ripples in shelf seas.' Continental Shelf Research 38, 47–62. (2012)